ACS OMEGA

http://pubs.acs.org/journal/acsodf

Article

A Highly Expanded Polycarboxylate Gel and New Environmental Response Effects for Efficiently Adsorbing and Recovering Cu(II) from Water

Hongyan Li,[#] Yu Bai,[#] Qiwen Yang, and Yikai Yu*

Cite This: *ACS Omega* 2021, 6, 5318−5334

Read Online

ACCESS | Metrics & More | Article Recommendations | Supporting Information

ABSTRACT: A new highly expanded polycarboxylate gel (EPCG) was accidentally formed in a facile cross-linking copolymerization system. When used as an adsorbent material, the EPCG could be quickly expanded 29.44 times in water to have a high permeability inside for realizing the efficient adsorption toward Cu(II) from water. The adsorption capacity of EPCG toward Cu(II) was 261.70 mg/g, which was higher than that of all the selected existing adsorbents reported in recent years. The adsorption rate of expanded EPCG was 3.61 times higher than that of the previous polyantionic gel. Similarly, due to the high expansion and high permeability of EPCG, the EPCG skeleton could be further coated with an alkaline NaOH, forming a novel NaOH-coated EPCG material, and its adsorption capacity toward Cu(II) was further improved to 333.21 mg/g compared to that of pure EPCG adsorbent. Moreover, the EPCG wastes after adsorbing Cu(II) could be fully desorbed to be regenerated for reuse. A total of 99.39% of the adsorbed Cu(II) was desorbed from EPCG wastes to be recovered. The adsorption capacity of regenerated EPCG reused for adsorbing Cu(II) was 259.05 mg/g, which was very near that of the original EPCG. In addition, a series of simulation experiments and instrumental analysis were adopted to confirm the new environmental response effects as the key factors in the purification of Cu(II)-containing wastewater, including "expansion-shrink," "alkali-coating," and "acid-desorption" responses.

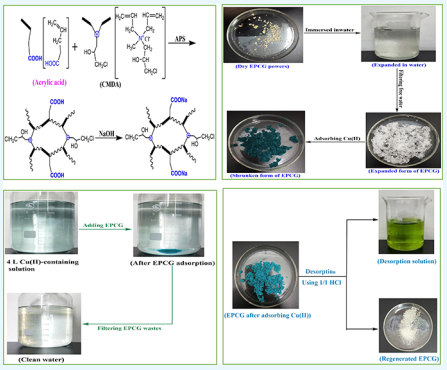

1. INTRODUCTION

Heavy-metal wastewater has caused serious environmental pollution and public health concerns, destroying the global sustainable development.[1−7] The copper of Cu(II) is considered to be one of the most common heavy-metal pollutants in wastewater from many industries, such as printed circuit, paint, copper polishing, electroplating, mining, smelting, petroleum refining, metal cleaning, fertilizer, and battery[8−12] The discharge of Cu(II)-containing wastewater will cause damage to the liver and heart and even lead to cancer, besides the serious pollution to the water environment. The World Health Organization (WHO) and the United State Environmental Protection Agency (USEPA) have ruled that the concentration of copper in drinking water should not exceed 1.5 and 1.3 mg/L, respectively.[13] To solve this problem, we should rely on effective wastewater treatment technologies.

There are many methods for treating the heavy-metal wastewater, such as adsorption, chemical precipitation, ion exchange, solvent extraction, and membrane filtration.[14−19] Of these, adsorption is one of the most widely used and simplest methods in the treatment of heavy-metal wastewater. The key is the selection of adsorption materials. At present, the adsorbent materials that can be used to adsorb Cu(II) in water mainly include inorganic adsorbent, organic adsorbent, and natural modified adsorbent.[20−25] However, the preparation process of the existing adsorbent materials is so expensive and complex, and some secondary pollution will be caused by their waste residues, thus limiting their wide application.[26−29]

Our work assumption was derived from a series of fundamental researches developing new water purification materials for treating various types of wastewater (e.g., heavy-metal wastewater, dyeing wastewater, and papermaking wastewater) in our past contributions.[30−35] In one of our previous contributions, we designed a novel polycarboxylate-based polyanionic gel (PAG) adsorbent material and discovered that it showed a higher adsorption capacity for Cu(II) than the existing adsorbent materials. For the reasons, the polycarboxylate skeletons of PAG could form strong complex bonds with Cu(II) so that the adsorption ability of PAG toward Cu(II) could improve.[36] In another previous contribution, we had noticed that the improvement of permeability of a gel adsorbent played an important role in enhancing its adsorption ability. A highly permeable

Received: November 6, 2020
Accepted: January 25, 2021
Published: February 18, 2021

https://dx.doi.org/10.1021/acsomega.0c05431
ACS Omega 2021, 6, 5318−5334

Scheme 1. A Work Assumption Expecting to Obtain the Highly Permeable Polycarboxylate Gel Based on Our Previous Fundamental Experiences

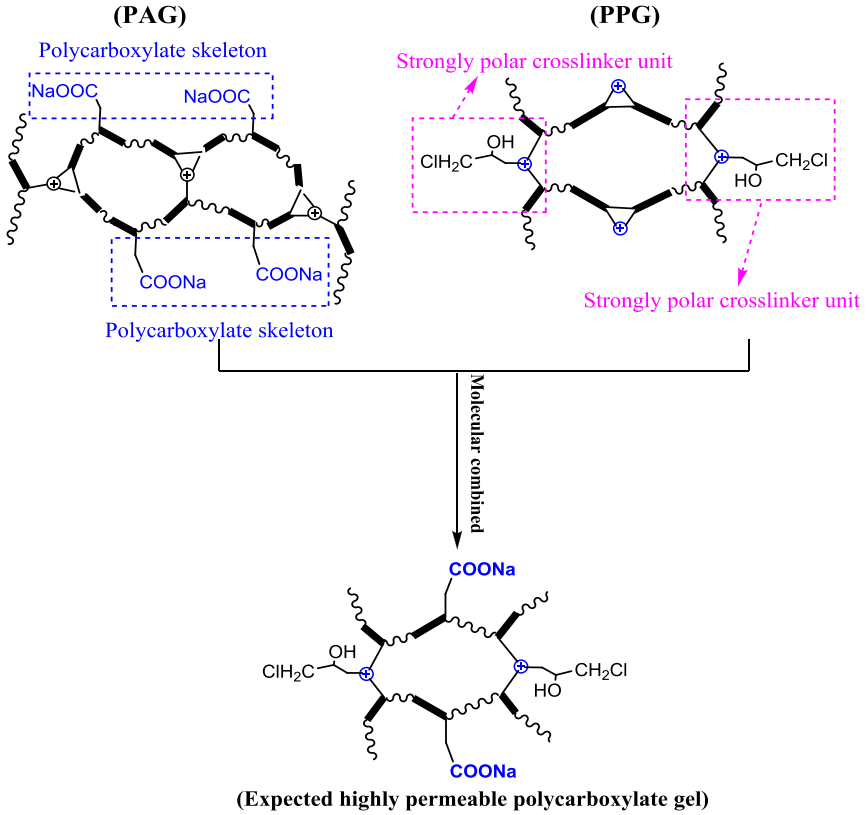

Scheme 2. Synthesis Route of the Target Polycarboxylate Gel Adsorbent

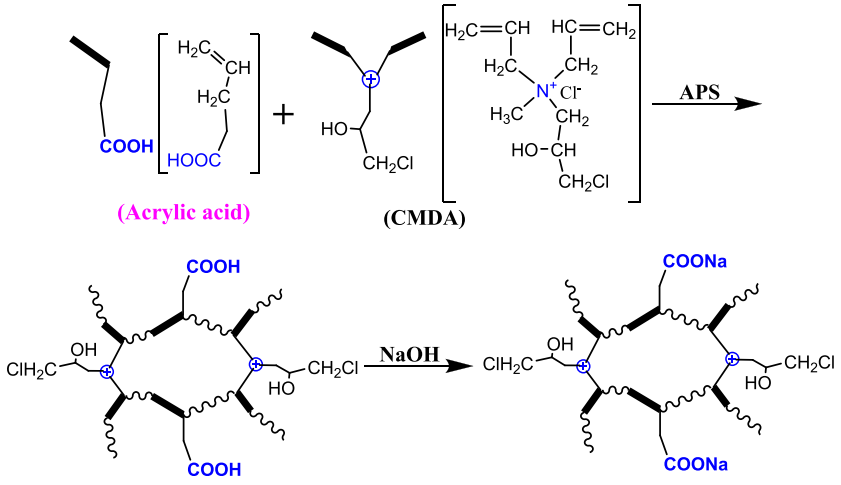

polycationic gel (PPG) had been obtained by incorporation of a strongly polar cross-linker unit into the gel skeleton, and the adsorption capacity of PPG was discovered to be improved 606.76 times higher than that of activated carbon.[37] We noticed that the strong polar cross-linker units and the hydrophilic cationic units could increase the water-swelling capacity of PPG, which provided larger accommodation spaces inside PPG so that the dyes could fully penetrate inside PPG to be efficiently absorbed. Thus, it could be considered that the high permeability of PPG had improved the absorption ability toward the dyes. These above-mentioned new previous fundamental findings had made us further believe that if the polycarboxylate skeletons (which could form strong complex bonds with Cu(II)) and the strongly polar cross-linker units (which could improve the permeability of a gel) were combined in a new gel molecular structure, a highly permeable polycarboxylate gel would be obtained (Scheme 1) and could be expected to be a more excellent adsorbent for treating the Cu(II)-containing wastewater more satisfactorily than we could do before.

In this work, combining our previous work experiences, we synthesized the designed highly permeable polycarboxylate gel by a facile cross-linking copolymerization of one cationic cross-linker with strong polar groups [i.e., 3-chloro-2-hydroxypropylmethyldiallylammonium chloride (CMDA)] and another common monomer of acrylic acid (AA) and then through a

https://dx.doi.org/10.1021/acsomega.0c05431
ACS Omega 2021, 6, 5318−5334

simple neutralization treatment (Scheme 2). The facile synthesis process had broken the current inconvenience of the other existing adsorbents regarding their complex and expensive preparation processes. To the interest, the obtained polycarboxylate gel adsorbent was accidentally found to be highly expanded in water. When immersed in water at the beginning, the obtained polycarboxylate gel could be quickly expanded 29.44 times [so we called it the highly expanded polycarboxylate gel (EPCG)] to have a high permeability inside for adsorbing the Cu(II) in water more efficiently than the existing adsorbents. After adsorbing the Cu(II), the volume of EPCG was shrunk again to enhance the adsorption strength of EPCG toward Cu(II). In the presence of alkali, the EPCG could be coated with hydroxyl ions, forming a novel NaOH-coated EPCG material with a higher adsorption capacity toward Cu(II) than that of the pure EPCG adsorbent. In the acid conditions, the EPCG samples with the saturated adsorption of Cu(II) could be fully desorbed to be regenerated for reuse, also realizing the high recovery of the Cu(II). Thus, the new environmental responses of EPCG to different conditions could be just the key factors for the EPCG to realize a more satisfactory adsorption toward Cu(II) than we could do before.

2. RESULTS AND DISCUSSION

2.1. Optimum Synthesis of the EPCG Adsorbent. As designed, the EPCG could be synthesized by a facile copolymerization of one cross-linker CMDA monomer and another acrylic acid (AA) monomer and then through a simple neutralization treatment. However, the optimum synthesis conditions should be preferentially confirmed to obtain the best EPCG product. To simultaneously take care of the effects of both CMDA and AA on the reaction results under the optimum synthesis conditions, we selected a representative copolymerization system in which the molar numbers of CMDA to AA were equal (i.e., the molar ratio of CMDA to AA was 50/50) to the model reaction object. To achieve the optimum conditions for EPCG synthesis, the effects of different reaction conditions [e.g., the reaction temperature (factor *A*), monomer concentration (factor *B*), APS initiator amount (factor *C*), and reaction time (factor *D*)] on the EPCG synthesis were systemically investigated according to an L_9 $(3)^4$ orthogonal experiment with four factors and three levels. The effects of each reaction condition were evaluated by the adsorption abilities of the EPCG products obtained from each condition. The results were shown in Table 1. The results showed that, when the reaction temperature was controlled as 90 °C, the monomer concentration was controlled as 50% (w/w), the APS initiator amount was controlled as 2% (w/w), and the reaction time was controlled as 5.0 h, the adsorption ability of the obtained EPCG adsorbent toward Cu(II) was stronger and achieved a higher Cu(II) removal percentage (*R*%) than the others; thus, the corresponding reaction conditions could be regarded as the optimum conditions for the EPCG synthesis.

To achieve the optimum synthesis conditions, the molecular structures of EPCG adsorbents were subsequently optimized by varying the molar ratios of CMDA to AA in the reaction systems from 5/95 to 100/0, and the results were shown in Figure 1. The results showed that the adsorption abilities of EPCG products were improved with the decrease of the molar ratios of CMDA to AA units in the molecular structures of EPCG because the decrease of the molar ratios of CMDA to AA units in the molecular structures meant the increase of the carboxylate contents (corresponding to the AA units) in the molecular structures of the corresponding EPCG, while the carboxylate units were just the critical units that could adsorb the Cu(II) in water, so the adsorption abilities of EPCG toward Cu (II) could be correspondingly improved in turn. When the molar ratio of CMDA to AA units in the molecular structures was controlled as 5/95, the adsorption ability of the corresponding EPCG product toward Cu(II) was the strongest to achieve the highest Cu(II) removal percentage (81.67%). Therefore, this EPCG product with the molar ratio of CMDA to AA units being 5/95 could be regarded as the optimum EPCG product for the next application in the purification of Cu(II)-containing wastewater.

Table 1. Orthogonal Experiments for the Optimum Synthesis of EPCG Adsorbents[a]

no.	*A* (°C)	*B* (w/w%)	*C* (w/w%)	*D* (h)	*R* (%)
1	70	45	2	3	24.60
2	70	50	3	4	20.32
3	70	55	4	5	31.28
4	80	45	3	5	34.49
5	80	50	4	3	26.20
6	80	55	2	4	30.48
7	90	45	4	4	34.76
8	90	50	2	5	37.17
9	90	55	3	3	35.56

[a]*A*: reaction temperature, *B*: monomer concentration, *C*: initiator amount, *D*: reaction time, and *R*%: Cu(II) removal percentage. Conditions for testing the adsorption abilities of EPCG products: 0.3 g of obtained EPCG products was used to adsorb 50 mL of 2000 mg/L Cu(II)-containing solution with continuous stirring at 30 °C for 100 h, and the Cu(II) removal percentage (*R*%) was used to evaluate the adsorption abilities of EPCG products, which could be calculated according to eq 1 shown in Section 2.3.

2.2. Environmental Responses of EPCG for Efficiently Adsorbing Cu(II) in Wastewater. When the EPCG adsorbent was used for treating Cu(II)-containing wastewater, it was found to be highly environmentally responsive, having an "expansion-shrink" response, "alkali-coating" response, and "acid-desorption" response.

2.2.1. Expansion-Shrink Response of EPCG Adsorption toward Cu(II) under Neutral Conditions. When the EPCG adsorbent was put into water, at the beginning, it could be quickly expanded (Figure 2). The expansion percentage (EP%) of EPCG in water was calculated according to the following equation:

$$\mathrm{EP\%} = \frac{W_1}{W_0} \times 100\% \quad (1)$$

where W_0 is the weight of the dry EPCG and W_1 is the weight of the expanded EPCG in water.

The calculation results via eq 1 showed that the expansion percentage (EP%) of EPCG in water could be calculated to be 2944% (Figure 2a vs c), i.e., the EPCG in water had been expanded 29.44 times higher than the dry EPCG. The high expansion response of EPCG in water might be derived from the following reasons: (1) Both the strong polar CMDA units and carboxylate units in the EPCG structures were hydrophilic, which was conducive to the swelling of EPCG in water. (2) After swelling, the isoelectric repulsion effects of carboxylate units would further make the internal structures of EPCG be

https://dx.doi.org/10.1021/acsomega.0c05431
ACS Omega 2021, 6, 5318−5334

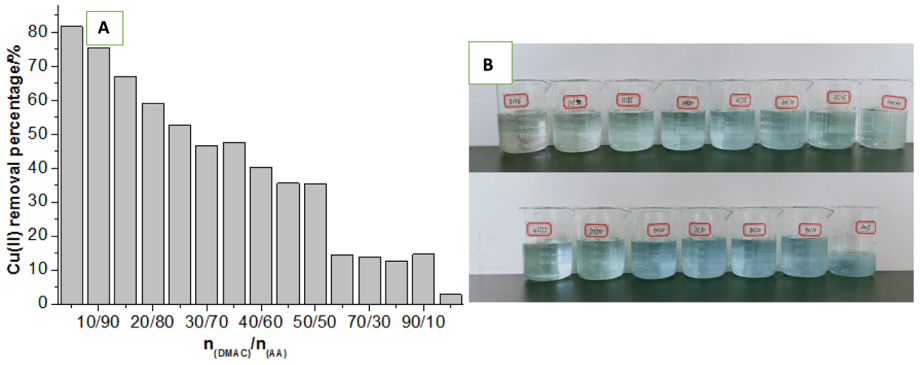

Figure 1. (a) The Cu(II) removal percentages from the adsorption of different molecular structures of EPCG products toward Cu(II). (b) The original photos of the adsorption results of different molecular structures of EPCG products toward Cu(II). Conditions for testing the adsorption abilities of EPCG products: 0.3 g of EPCG products was used to adsorb 50 mL of 2000 mg/L Cu(II)-containing solution with continuous stirring at 30 °C for 100 h, and the adsorbed solutions were filtered to measure the adsorption results. The Cu(II) removal percentages (R%) could be calculated according to eq 1 shown in Section 2.3.

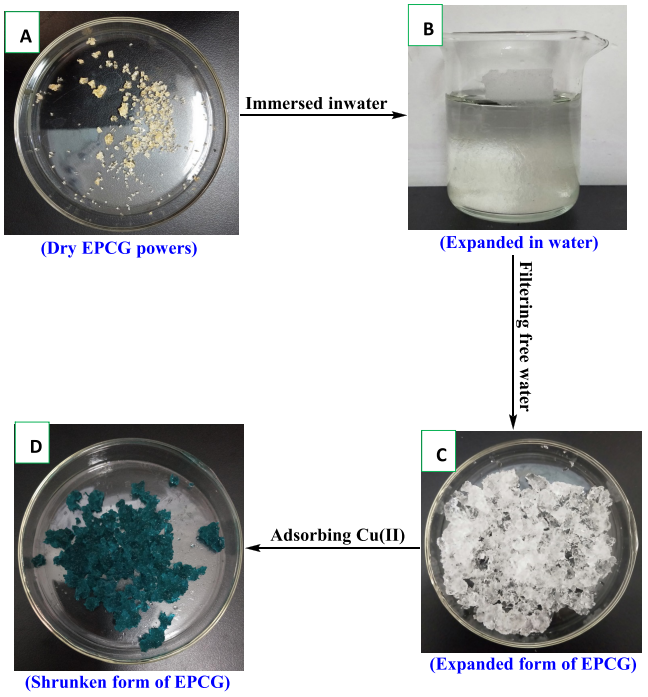

Figure 2. (a) The original photo of the form of dry EPCG powers (0.5 g). (b) The original photo of the form of EPCG (0.5 g) expanded in 50 mL of deionized water. (c) The original photo of the final expanded form of EPCG (0.5 g) after filtering the free water. (d) The original photo of the form of EPCG wastes after 0.5 g of EPCG adsorbed 50 mL of 2000 mg/L Cu(II)-containing solution.

expanded. The high expansion of EPCG in water would provide a high permeability inside EPCG to adsorb the Cu(II) in water, so the Cu(II) in water could be efficiently adsorbed by the EPCG adsorbent. After adsorbing the Cu(II), the volumes of EPCG adsorbents were shrunk again (Figure 2c vs d). This might be because the isoelectric repulsion effects of carboxylate units disappeared and the carboxylate units of EPCG had been combined with the Cu(II) to form a complex structure. The shrinking of EPCG after adsorbing the Cu(II) would enhance the adsorption strength of EPCG toward Cu(II).

We measured the adsorption rate and adsorption capacity of EPCG toward Cu (II) in water to evaluate the adsorption ability of EPCG for treating the Cu (II)-containing wastewater, and the results were shown in Figure 3. We selected the expanded EPCG samples containing 0.1 g of pure EPCG weight to adsorb the 50 mL of 2000 mg/L Cu(II)-containing solution for 1−10 min, respectively, to investigate the adsorption results of expanded EPCG products at different adsorption times (Figure 3a). It took only 3 min for the expanded EPCG to adsorb Cu(II) to achieve the adsorption equilibrium. The adsorption rate (AR) of the expanded EPCG toward Cu(II) could be calculated according to the following equation:

$$\mathrm{AR} = \frac{(C_0 = C_t) \times V}{mt} \tag{2}$$

where C_0 is the original Cu(II) concentration in the solution (2000 mg/L), C_t is the Cu (II) concentration in the solution after EPCG adsorption at time t, V is the volume of the selected Cu(II)-containing solution, m is the mass of the used EPCG adsorbent, and t is the adsorption time.

The calculation results via eq 2 showed that the average adsorption rate (AR) of expanded EPCG toward Cu (II) before the adsorption equilibrium (i.e., at the time interval of 1−3 min) was calculated to be 95.83 mg·g^{-1}·min^{-1}, which was 3.61 times higher than that of the similar polyantionic gel (PAG) reported in our previous contribution (according to the same calculation method, the adsorption rate of PAG toward Cu(II) at the corresponding time interval of 1−3 min could be calculated to be 26.57 mg·g^{-1}·min^{-1}) (Figure 3b). This indicated that the adsorption rate of EPCG after being expanded had been greatly accelerated.

The adsorption data of expanded EPCG at different adsorption times were further substituted into the serial adsorption kinetic equations shown as eqs 3−6 to investigate the adsorption kinetic behaviors of expanded EPCG (Figure 3c−f).

$$\log(q_e - q_t) = \log q_e - \frac{k_1 t}{2.303} \tag{3}$$

$$\frac{t}{q_t} = \frac{1}{k_2 q_e^{\,2}} + \frac{t}{q_e} \tag{4}$$

$$q_t = k_i t^{1/2} + x_i \tag{5}$$

https://dx.doi.org/10.1021/acsomega.0c05431
ACS Omega 2021, 6, 5318−5334

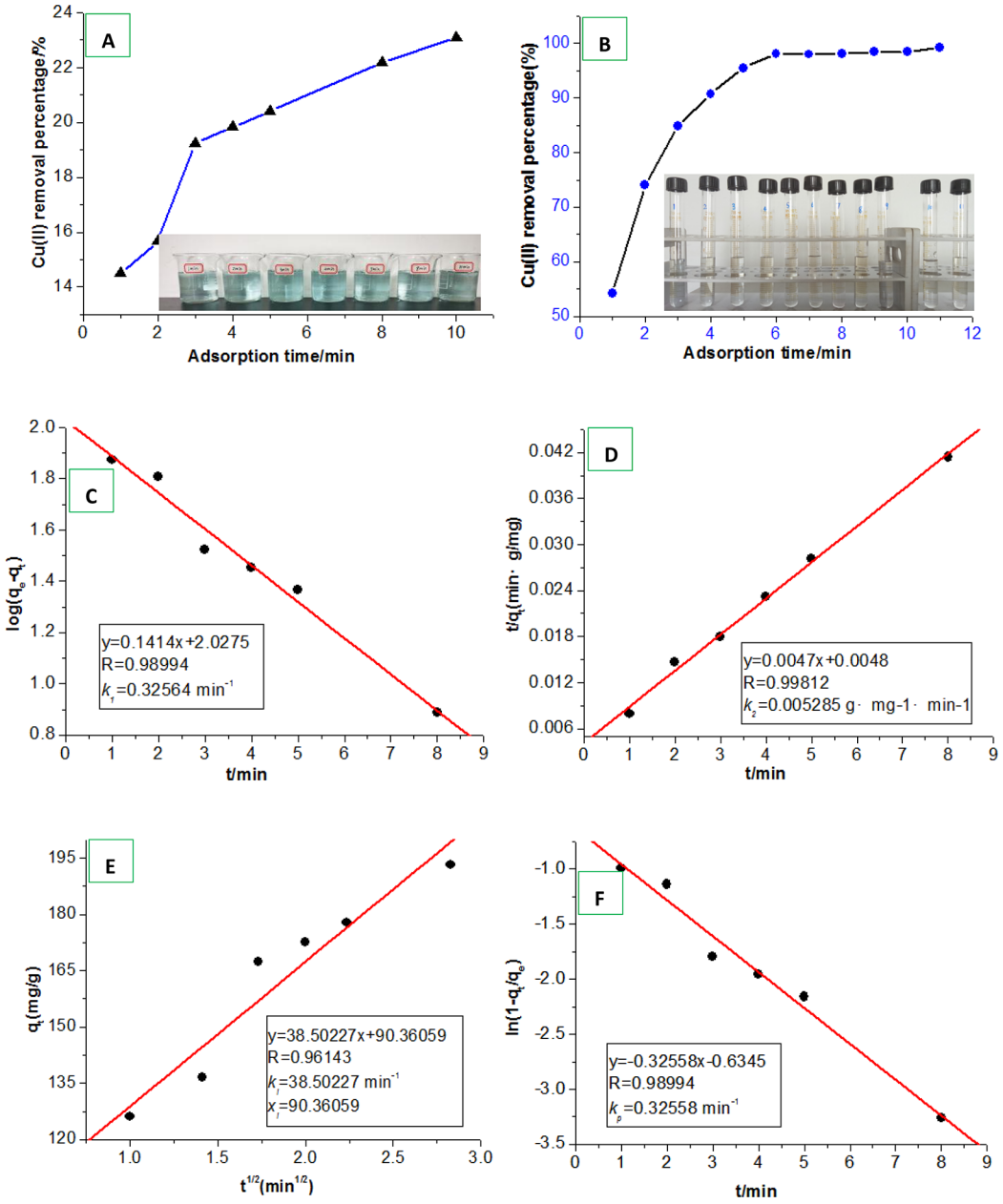

Figure 3. (a) The adsorption results of EPCG at different adsorption times (1−10 min). The original photo was further used to track the adsorption results of EPCG toward Cu(II) at the corresponding adsorption time. (b) The adsorption results of PAG toward Cu(II) at different adsorption times, which were derived from ref 36. (c) Fitting the pseudo-first kinetics model equation using adsorption data of EPCG toward Cu(II). (d) Fitting the pseudo-second kinetics model equation using adsorption data of EPCG toward Cu(II). (e) Fitting the intraparticle diffusion model equation using adsorption data of EPCG toward Cu(II). (f) Fitting the particle diffusion model equation using adsorption data of EPCG toward Cu(II).

Table 2. Comparison of the Adsorption Kinetics Constants of EPCG and PPG

adsorbent	adsorbate	k_1 (min^{-1})	k_2 ($g{\cdot}mg^{-1}{\cdot}min^{-1}$)	k_p (min^{-1})	x_i	k_i ($mg{\cdot}g^{-1}{\cdot}min^{1/2}$)	ref.
PPG	Cu(II)	0.13	0.000313	0.13	83.13	45.05	36
EPCG	Cu(II)	0.33	0.000529	0.33	90.36	38.50	this work

$$\ln\left(1 - \frac{q_t}{q_e}\right) = -k_p t \quad (6)$$

where k_1, k_2, k_i, and k_p stood for the adsorption rate constants corresponding to the pseudo-first kinetics, pseudo-second kinetics, intraparticle diffusion, and particle diffusion equations, respectively.

The results showed that the adsorption of expanded EPCG well accorded with all of the selected pseudo-first kinetics, pseudo-second kinetics, intraparticle diffusion, and particle diffusion model equations because the correlation coefficients in the case were above 0.96, indicating that the adsorption of expanded EPCG toward Cu(II) was achieved through a combined adsorption process. Moreover, the adsorption rate

https://dx.doi.org/10.1021/acsomega.0c05431
ACS Omega 2021, 6, 5318−5334

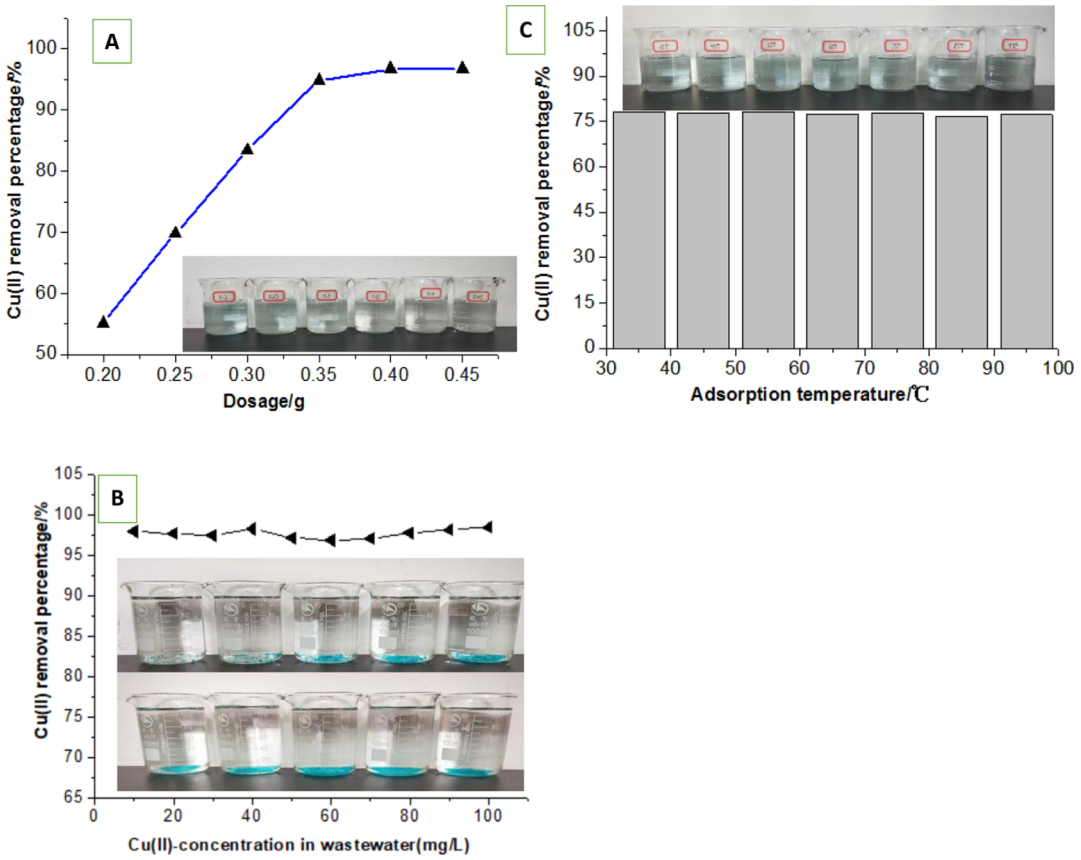

Figure 4. (a) The adsorption results of different dosages of EPCG toward 2000 mg/L Cu(II)-containing solution. (b) Adsorption results of EPCG toward 10−100 mg/L Cu(II)-containing wastewater. The original adsorption effects at each condition could be correspondingly tracked in photos. Adsorption conditions: the same mass ratio of PAG to Cu(II) in wastewater (1:250 g/mg) was used to calculate suitable EPCG dosages, and the calculated dosages of EPCG were used to adsorb 100 mL of 10−100 mg/L Cu(II)-containing wastewater. (c) Effect of different adsorption temperatures on adsorption of EPCG toward Cu(II). Test conditions: 0.3 g of EPCG samples was added to adsorb 50 mL of 2000 mg/L Cu(II)-containing solution with continuous stirring at 35−95 °C for 100 h, respectively.

constants of expanded EPCG corresponding to the pseudo-first kinetics (k_1 = 0.33 min^{-1}), pseudo-second kinetics (k_2 = 0.000529 $g{\cdot}mg^{-1}{\cdot}min^{-1}$), and particle diffusion equations (k_p = 0.33 min^{-1}) were, respectively, 2.51, 1.69, and 2.51 times higher than those of the similar polyantionic gel (PAG) reported in our previous contribution (k_1 = 0.13 min^{-1}, k_2 = 0.000313 $g{\cdot}mg^{-1}{\cdot}min^{-1}$, and k_p = 0.13 min^{-1}) (Table 2), which would be the key factors for the expanded EPCG to achieve a higher adsorption rate.

Figure 4a showed the adsorption results of EPCG toward the 50 mL of 2000 mg/L Cu(II)-containing solution with different dosages of EPCG (0.20−0.50 g). The results showed that the Cu (II) removal percentages for EPCG adsorption were increased with the increase of EPCG dosages from 0.20 to 0.30 g, indicating a saturated adsorption state at the EPCG dosages of 0.20−0.35 g. However, when the EPCG dosages were above 0.35 g, the Cu(II) removal percentages for EPCG adsorption maintained an ultimate limit level and changed a little, indicating that the EPCG dosages were excessive. The maximal adsorption capacity (Q_{max}) for EPCG adsorption was represented by the average values of the equilibrium adsorption capacities (q_e) under the saturated adsorption states with the EPCG dosages being 0.20−0.35 g. The results showed that the maximal adsorption capacity (Q_{max}) of EPCG adsorption was calculated to be 261.70 mg/g, which was higher than that of most of the selected existing adsorbents reported in the recent years[28,30−51] and was also lower than that of a few existing adsorbents[49,60] (Table 3). However, the existing adsorbent materials are usually difficult to prepare due to the complex and expensive preparation process, or some of them are likely to cause another waste disposal problem after the water treatment process.[38−60] In contrast, the EPCG preparation process was very facile, which was only through a facile cross-linking copolymerization and then a simple neutralization treatment. Therefore, on the whole, the EPCG adsorbent would be superior to the existing adsorbent materials in the purification of Cu(II)-containing wastewater.

We further used the EPCG adsorbents to treat the low-Cu(II)-concentration (10−100 mg/L) wastewater, and the results were shown in Figure 4b. The results showed that when the mass ratios of the EPCG to the Cu(II) in the wastewater with different Cu(II) concentrations were the same at 1/250 g/mg, the Cu(II) removal percentages were within the relatively stable ranges of 97.1−98.5%, which were very near the value when treating the 2000 mg/L of Cu(II)-containing wastewater under the same testing conditions (see Figure 4a), indicating the adsorption abilities of EPCG toward wastewater with different Cu(II) concentrations. Thus, the EPCG adsorbents were very suitable to treat the wide Cu(II)-concentration ranges (10−2000 mg/L) of Cu(II)-containing wastewater.

https://dx.doi.org/10.1021/acsomega.0c05431
ACS Omega 2021, 6, 5318−5334

Table 3. Comprehensive Comparison of the Adsorption Capacity of EPCG Products to Those of the Serial Existing Adsorbents Reported in the Recent Years[a]

adsorbent	adsorbate	Q_{max} ($mg \cdot g^{-1}$)	reference
CNF-supported cryogels	Cu(II)	138.0	38
functionalized polyacrylonitrile fiber	Cu(II)	141.7	39
magnetic calcium alginate hydrogel bead	Cu(II)	159.2	40
cellulose-graft-polyacrylamide/hydroxyapatite composite hydrogel	Cu(II)	179.0	40
polyurethane foam and rice straw	Cu(II)	193.6	41
multifunctional nitrogen-doped carbon	Cu(II)	214.0	41
laterite	Cu(II)	7.249	42
electrospun DTPA-modified chitosan/polyethylene oxide nanofibers	Cu(II)	177	43
mesoporous composite material	Cu(II)	197.15	44
poly(ammonium/pyridinium)-chitosan Schiff base	Cu(II)	98.9	45
phytic acid functionalized spherical poly-phenylglycine particles	Cu(II)	90.5	46
ligand functionalized composite material	Cu(II)	171.33 mg/g	47
polysaccharide-constructed hydrogels	Cu(II)	107.2	48
Mg/Fe layered double hydroxide with Fe3O4-carbon spheres	Cu(II)	388.77	49
hydrophilic P(Am-CD-AMPS) microgel	Cu(II)	85.00	50
aminated polyacrylonitrile nanofibers	Cu(II)	149.8	51
mesoporous conjugate material	Cu(II)	183.81	52
chelating resin	Cu(II)	78.08	53
biochar	Cu(II)	4−5	54
functionalized graphene nanosheet	Cu(II)	103.22	55
hollow polymer nanoparticle	Cu(II)	145.14	56
ZIF-8	Cu(II)	98.63	57
hydroxyapatite/biochar nanocomposite	Cu(II)	99.01	58
carnauba straw powder	Cu(II)	9.50	59
Ca−Al layered double hydroxide	Cu(II)	444.5	60
PAG	Cu(II)	222.20	36
EPCG	Cu(II)	261.70	This work

[a]The optimum PAG products with the suitable molar ratios of DMAC and AA units of 5/95 were selected to be compared.

In addition, Figure 4c showed that when the adsorption temperatures were varied from 35 to 95 °C, the Cu(II) removal percentages from the adsorption of EPCG toward Cu(II) were almost unchanged, further indicating that strong adsorption interactions had been formed between EPCG and Cu(II).

Generally, the expansion-shrink response of EPCG had improved the adsorption rate, adsorption capacity, and adsorption strength for removing the Cu(II) in water, thus realizing a more satisfactory purification of the Cu(II)-containing wastewater than we could do before.

2.2.2. Alkali-Coating Response of EPCG to Improve the Ability for Purifying Cu(II)-Containing Wastewater. Similarly, due to the high expansion and high permeability of EPCG, when the EPCG adsorbent was added into an alkaline NaOH solution, driven by an internal and external concentration difference, the NaOH regents would be permeated inside the expanded EPCG to be coated by EPCG skeletons, forming a novel NaOH-coated EPCG product. We investigated the effects of different coating conditions on the abilities of NaOH-coated EPCG products to remove Cu(II) through an L_9 $(3)^3$ orthogonal experiment with three factors and three levels (Table 4). The results showed that when the coating temperature was 80 °C, the concentration of the NaOH solution was 3% (w/w), and the coating time was 2.0 h. The removal result of the obtained NaOH-coated EPCG toward Cu(II) was the best, so the corresponding coating conditions could be regarded as the optimal coating conditions.

Table 4. Optimum Conditions for the Formation of NaOH-coated EPCG Products[a]

no.	*A* (%)	*B* (°C)	*C* (h)	Cu(II) removal percentage (%)
1	1	70	2	67.44
2	1	80	3	65.87
3	1	90	4	64.02
4	2	70	3	97.88
5	2	80	4	98.15
6	2	90	2	92.33
7	3	70	4	93.12
8	3	80	2	99.21
9	3	90	3	99.21

[a]*A*: the concentration of NaOH solution, *B*: coating temperature, and *C*: coating time. The weight ratio of EPCG to the NaOH solution was 1:30. Conditions for testing the Cu(II) removal percentages using NaOH-coated EPCG products: 0.3 g of NaOH-coated EPCG products was stirred with 50 mL of 2000 mg/L Cu(II)-containing solution at 30 °C for 100 h and then filtered to measure the Cu(II)-concentration residual in the solution and calculate the Cu(II) removal percentages according to eq 9 shown in the subsequent Section 4.3.

Subsequently, different dosages (0.05−0.30 g) of NaOH-coated EPCG products were added to treat 50 mL of 2000 mg/L Cu(II)-containing solution at 30 °C for 100 h (Figure 5)

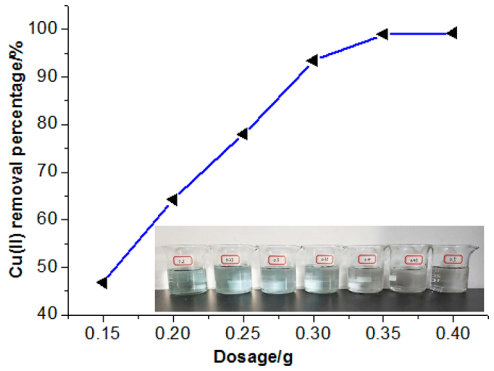

Figure 5. The interaction results of different dosages of NaOH-coated EPCG products toward Cu(II).

to evaluate the ability of the optimal NaOH-coated EPCG for removing Cu(II). The results showed that the adsorption and precipitation of NaOH-coated EPCG had taken place at the same time to be interacted with Cu(II) (Scheme 3). The ability of NaOH-coated EPCG to remove Cu(II) was evaluated using the mass of Cu(II) removed per gram of NaOH-coated EPCG (R_{Cu}, mg/g), which could be calculated by the average values of the saturated interaction states with the dosages of NaOH-coated EPCG being 0.05−0.20 g. The

https://dx.doi.org/10.1021/acsomega.0c05431
ACS Omega 2021, 6, 5318−5334

Scheme 3. The Interaction Mechanisms between the NaOH-coated EPCG Product and Cu(II)

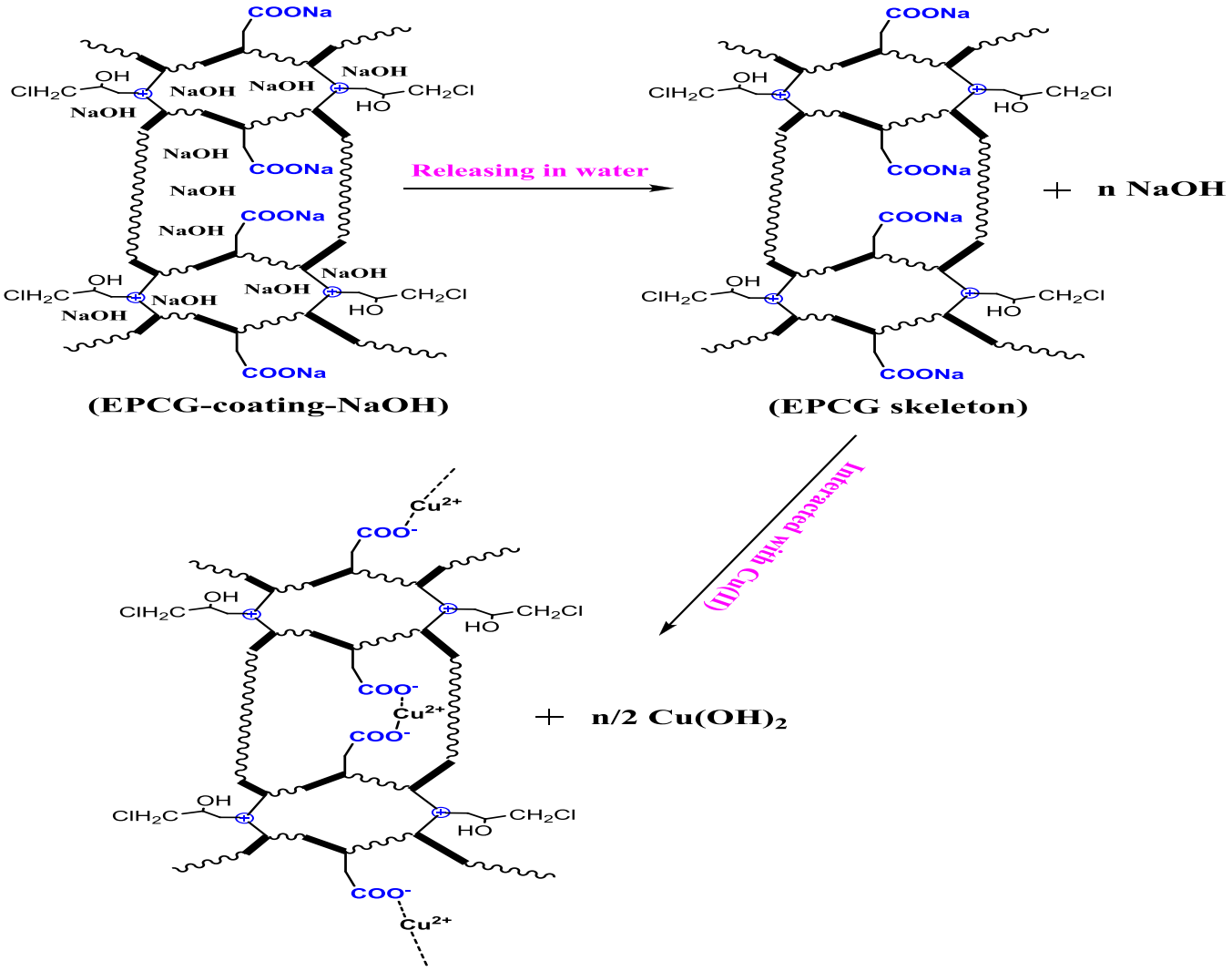

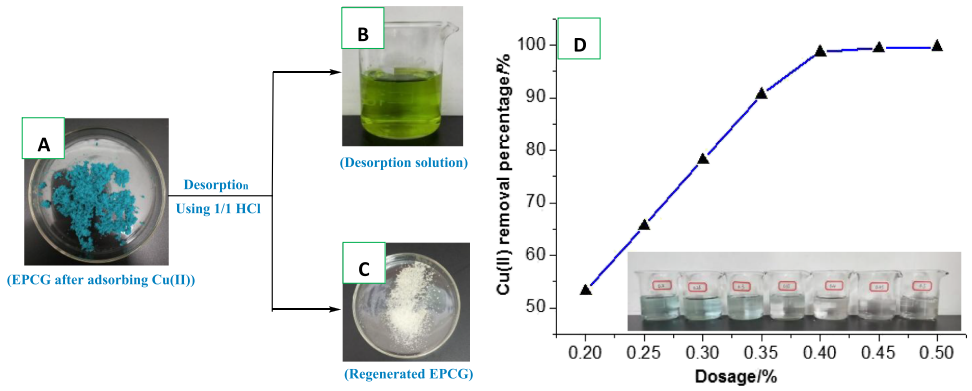

Figure 6. (a) The EPCG samples with the saturated adsorption of Cu(II). (b) The original photo of the desorption solution. (c) The original photo of the regenerated EPCG samples. (d) The adsorption results of different dosages of regenerated EPCG adsorbents toward Cu(II).

R_{Cu} of NaOH-coated EPCG was calculated as 333.21 mg/g, which was greatly improved in comparison with the adsorption capacity of the pure EPCG adsorbent. Thus, the ability of NaOH-coated EPCG to remove Cu(II) had been greatly improved in comparison with the pure EPCG adsorbent.

2.2.3. Acid-Desorption Response of EPCG to Realize the Regeneration and Reuse. In the acid conditions, the EPCG samples with the saturated adsorption of Cu(II) could be efficiently desorbed to be regenerated for reuse, and the desorbed Cu(II) could be recovered. At room temperature, when 0.3 g of EPCG samples with the saturated adsorption of Cu(II) (Figure 6a) was stirred with a 50 mL 1/1 (v/v) HCl solution for 100 h, most of the adsorbed Cu(II) had been desorbed from the EPCG skeletons to be soluble in the HCl

https://dx.doi.org/10.1021/acsomega.0c05431
ACS Omega 2021, 6, 5318−5334

Scheme 4. The Desorption Mechanism of EPCG Samples with the Saturated Adsorption of Cu(II)

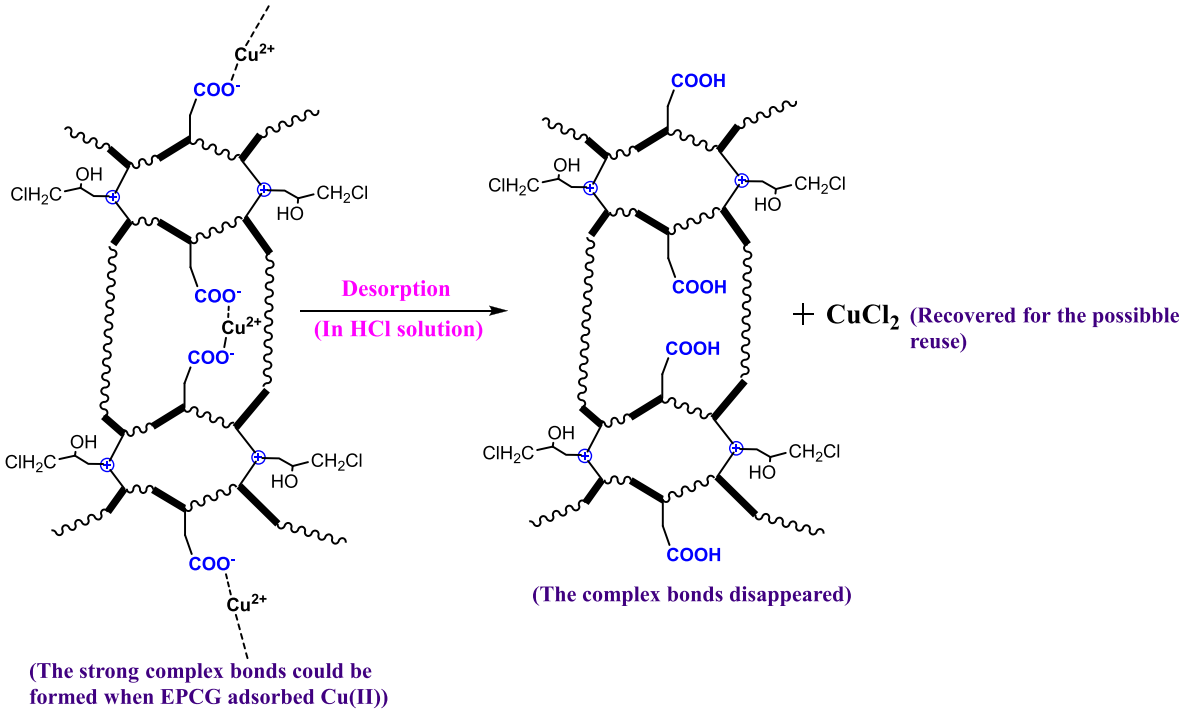

solution (Figure 6b), and the EPCG samples after desorption had no difference in the exterior colors from the original EPCG samples (Figure 6a vs c). The Cu(II) contents in the EPCG skeletons before and after desorption could be confirmed by the X-ray photoelectron spectroscopy (XPS), and the Cu(II) desorption percentage (DR%) was calculated by the following equation:

$$\mathrm{DR\%} = \left(1 - \frac{x_1}{x_0}\right) \times 100\% \tag{7}$$

where x_0 is the Cu(II) content before desorption and x_1 is the Cu(II) content after desorption.

The calculation result via eq 7 showed that the Cu(II) desorption percentage (DR%) was 99.39%, i.e., 99.39% of the adsorbed Cu(II) could be desorbed to be recovered, confirming the efficient desorption of Cu(II) from the EPCG skeletons in the acid conditions. The interaction mechanism for realizing the efficient desorption of EPCG samples with the saturated adsorption of Cu(II) could be explained as follows: In the acid conditions, H^+ could be combined with the $-COO^-$ groups of EPCG skeletons, which would destroy the complex interactions between the Cu(II) and -COO^- groups of EPCG skeletons so that the Cu(II) ions became freer to be soluble in the desorption solution, thus realizing the efficient desorption of Cu(II) from the EPCG skeletons (Scheme 4). The efficient adsorption and desorption characteristics of EPCG adsorbents meant a good possibility for using EPCG adsorbents to realize the efficient recovery of Cu(II) from wastewater in future works: First, the Cu(II) could be well extracted from the Cu(II)-containing wastewater based on the efficient adsorption characteristic of EPCG toward Cu(II). Subsequently, the Cu(II) adsorbed by EPCG skeletons could be released again into a specific desorption solution to be recovered for possible reuse based on the efficient desorption characteristic of EPCG.

The EPCG samples after desorption were re-neutralized with a NaOH solution to regenerate the EPCG adsorbents for reuse. The regenerated EPCG adsorbents were reused to adsorb the Cu(II)-containing solution, and the results were shown in Figure 6d. Based on the adsorption results of regenerated EPCG in Figure 6d, we calculated the maximal adsorption capacity (Q_{max}) of regenerated EPCG by the average values of the equilibrium adsorption capacities (q_e) under the saturated adsorption states with the dosages being 0.05−0.20 g. The Q_{max} of regenerated EPCG was calculated as 259.05 mg/g, which was very near that of the original EPCG, indicating that the EPCG adsorbent could be efficiently recycled for reuse in the purification of Cu(II)-containing wastewater.

2.3. Enlarged Application of EPCG Adsorption for Purifying Cu(II)-Containing Wastewater. Corresponding to the conditions of small-scale breaker experiments of EPCG adsorption toward Cu(II) (see Figure 5), we enlarged the application scale in equal proportions for 40 times to investigate the enlarged application properties of EPCG in the purification of Cu(II)-containing wastewater. In this case, 1.6 g of EPCG adsorbents was added to adsorb 4.0 L of 100 mg/L Cu(II)-containing solution with continuous stirring for 100 h, and the results were shown in Figure 7. The results showed that under the enlarged application conditions, the EPCG adsorbents also showed excellent adsorption abilities so that the 4.0 L Cu(II)-containing solution became very clear. The Cu(II) removal percentage in the enlarged application was 98.2%, which was very near that of the corresponding breaker experiment when 0.40 g of EPCG products was used to adsorb 100 mL of 100 mg/L Cu(II)-containing solution (Figure 5 vs Figure 7c), indicating that the application properties of EPCG

https://dx.doi.org/10.1021/acsomega.0c05431
ACS Omega 2021, 6, 5318−5334

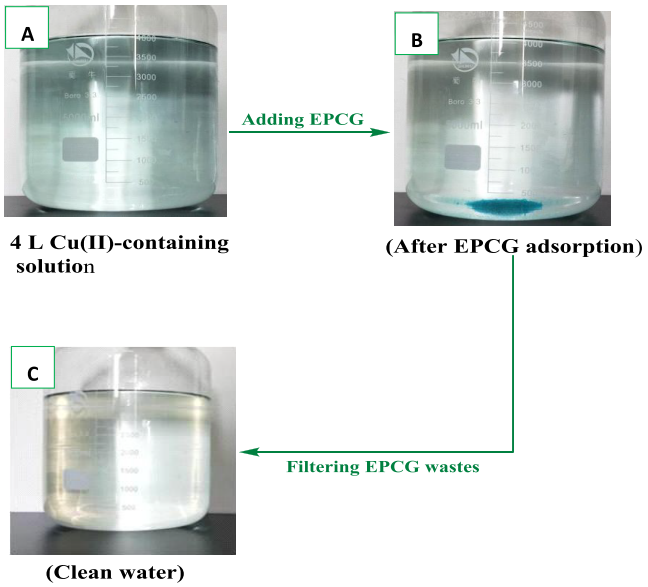

Figure 7. (a) The original photo of the 4.0 L of 100 mg/L Cu(II)-containing solution. (b) The adsorption results of 1.6 g EPCG adsorbents toward the 4.0 L of 100 mg/L Cu(II)-containing solution. (c) The final state of clean water after filtering the EPCG wastes.

adsorbents were stable in the enlarged application. Thus, in the future, this new EPCG adsorbent would have a good potential to be further applied in real engineering for purifying Cu(II)-containing wastewater.

2.4. Microstructure Transformations from the Environmental Responses of EPCG Adsorptions. A series of instrumental analysis technologies [e.g., Fourier transform infrared spectrum (FT-IR, Nicolet FT-IR (510 P, USA) spectrophotometer), scanning electron microscope (SEM,JSM-5610 SEM instrument), X-ray diffraction (XRD, Rigaku D/MAX-IIA X-ray diffractometer), and X-ray photoelectron spectroscopy (XPS, Thermo VG multilab 2000 spectrometer)] were adopted to detect the microstructure transformations of EPCG to confirm the environmental responses of EPCG adsorbents when adsorbing Cu(II). The results were shown in Figures 8−12, respectively.

The FT-IR spectra in Figure 8i showed the molecular structure transformations during the EPCG adsorptions. A characteristic absorption peak of −COONa at 1585 cm^{-1} (peak 1) could be clearly observed in the FT-IR spectra of the original EPCG sample (curve ″a″ in Figure 8i), exhibiting a sodium polyacrylate skeleton in the EPCG molecular structure. After adsorbing Cu(II), the outline of the absorption curve of the EPCG sample at 771−1410 cm^{-1} (peak 2) became very different from that of the original EPCG sample (curve ″a″ vs ″b″ in Figure 8i), the characteristic absorption peak of −COONa was shifted to 1545 cm^{-1} (peak 3), and a new absorption peak at 1716 cm^{-1} (peak 4) was further formed, all of which indicated that the molecular structures of EPCG had greatly changed after adsorbing Cu(II), possibly because a new EPCG−Cu(II) complex structure could be formed after EPCG adsorbed Cu(II). For the regenerated EPCG sample, its FT-IR absorption curve was very similar to that of the original EPCG sample (curve ″a″ vs ″c″ in Figure 8i), indicating that the regenerated EPCG had been recovered to the previous molecular structure of the original EPCG, thus having a highly efficient recyclability to be reused. Compared to the absorption curve of NaOH-coated EPCG before being interacted with Cu(II) (curve ″d″ in Figure 8i), the FT-IR curve of NaOH-coated EPCG after being interacted with Cu(II) (curve ″e″ in Figure 8i) showed a new absorption peak at 602 cm^{-1} (peak 5), the absorption intensity of EPCG skeleton had been weakened at 862 cm^{-1} (peak 6), and the absorption intensities of EPCG skeleton at 1054−2922 cm^{-1} (peak 7) became stronger. The molecular changes of the NaOH-coated EPCG samples before and after being interacted with Cu(II) suggested that efficient interactions had been formed between NaOH-coated EPCG and Cu(II) in the purification of Cu(II)-containing wastewater.

The XRD analysis in Figure 8ii revealed the changes of crystalline structures of EPCG in the purification of Cu(II)-containing wastewater. After EPCG adsorbed Cu(II), the diffraction peak of $2\theta = 7.73°$ was absent (curve ″a″ vs ″b″ in Figure 8ii), showing that the crystalline structures for EPCG adsorbed Cu(II). Meanwhile, for the regenerated EPCG sample, its XRD curve was very similar to that of the original EPCG sample (curve ″a″ vs ″c″ in Figure 8ii), further confirming that the regenerated EPCG had been recovered to the previous molecular structure of the original EPCG, which was in accordance with the previous FT-IR analysis results (see curve ″a″ vs ″c″ in Figure 8ii). However, there were almost no diffraction peaks shown in the XRD curve of NaOH-coated EPCG (curve ″d″ in Figure 8ii), possibly because the diffraction peaks of EPCG skeletons were blocked by the coated NaOH. When the NaOH-coated EPCG samples were

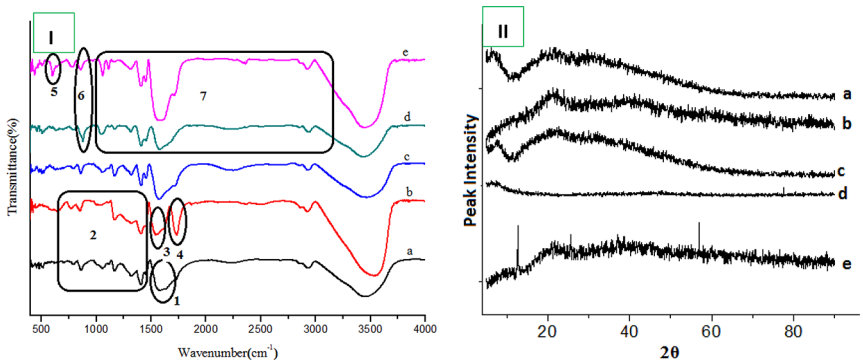

Figure 8. (i) FT-IR analysis of EPCG samples before (a) and after (b) adsorbing Cu(II), the regenerated EPCG samples (c), and the NaOH-coated EPCG products before (d) and after (e) being interacted with Cu(II). (ii) XRD analysis of EPCG samples before (a) and after (b) adsorbing Cu(II), the regenerated EPCG samples (c), and the NaOH-coated EPCG samples before (d) and after (e) being interacted with Cu(II).

https://dx.doi.org/10.1021/acsomega.0c05431
ACS Omega 2021, 6, 5318−5334

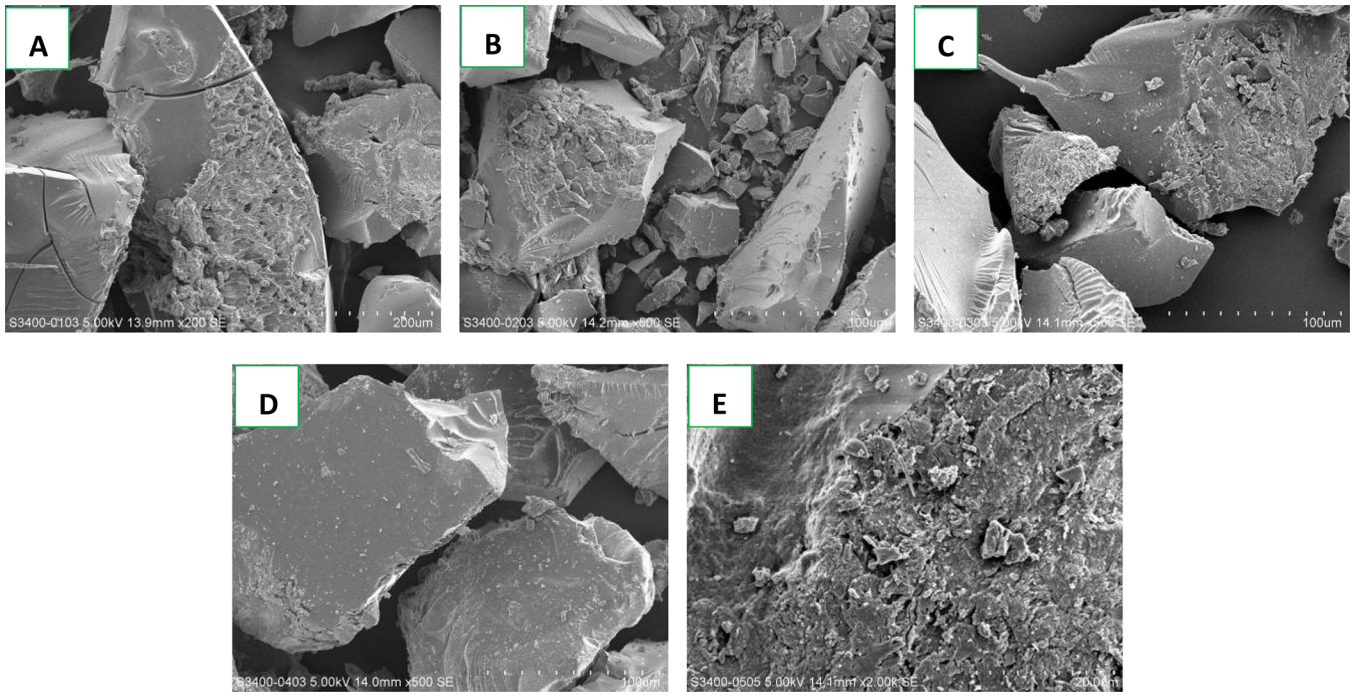

Figure 9. SEM analysis of EPCG samples before (a) and after (b) adsorbing Cu(II), the regenerated EPCG samples (c), and the NaOH-coated EPCG products before (d) and after (e) being interacted with Cu(II).

interacted with Cu(II), the diffraction peaks of EPCG skeletons reappeared, which were similar to those of the EPCG samples after adsorbing Cu(II) (curve ″b″ vs ″e″ in Figure 8ii), suggesting that the EPCG skeletons in the NaOH-coated EPCG system efficiently adsorbed Cu(II). Moreover, some spikes were further observed in curve ″e″ of Figure 8ii, which could be attributed to the formation of $Cu(OH)_2$. Thus, the XRD analysis further demonstrated that efficient interactions had been formed between EPCG (or NaOH-coated EPCG) and Cu(II) in the purification of Cu(II)-containing wastewater.

The SEM analysis in Figure 9 showed the changes of morphological structures of EPCG before and after adsorbing Cu(II). The results showed that the original EPCG sample exhibited a rough surface (Figure 9a). The general particle sizes of EPCG after adsorbing Cu(II) were smaller than those of original EPCG (Figure 9a vs b), which could be attributed to the shrinking effects of EPCG when adsorbing Cu(II). The surface morphologies of regenerated EPCG were similar to those of the original EPCG (Figure 9a vs c), further confirming that the EPCG products could be well regenerated for recycling reuse. Compared to the original EPCG samples, the surfaces of NaOH-coated EPCG samples were smoother (Figure 9a vs d); possibly, the coating effects of NaOH filled the EPCG surfaces. Moreover, after being interacted with Cu(II), some small particles were embedded onto the sample surfaces (Figure 9d vs e), which could be attributed to the formation of insoluble $Cu(OH)_2$ precipitations between the NaOH in NaOH-coated EPCG and the Cu(II), so realizing the further removal of Cu(II) besides the EPCG skeletons could efficiently adsorb Cu(II). Thus, it could be further concluded from the SEM analysis that efficient interactions had been formed between EPCG (or NaOH-coated EPCG) and Cu(II) in the purification of Cu(II)-containing wastewater.

Compared with the XPS analysis results of EPCG samples before and after adsorbing Cu(II) in Figures 10 and 11, the binding energies of carboxylic groups changed greatly. First, the C 1s binding energies of C−O and C═O shifted positively from 286.16 and 287.95 eV to 286.31 and 288.17 eV, while the C 1s binding energy of O−C═O shifted negatively from 289.45 to 288.86 eV. Secondly, the O 1s binding energies of C−O and C═O shifted positively from 532.79 and 531.23 eV to 533.44 and 531.84 eV, indicating that the O 1s binding energies were strengthened after EPCG adsorbed Cu(II), which could be attributed to the strong complex interactions formed between the carboxylic groups of EPCG and Cu(II) for the adsorption of EPCG toward Cu(II). Moreover, after adsorbing Cu(II), the peak of the Na 1s binding energy was almost absent (Figure 10e vs Figure 11e), but the new peak of the Cu $2p^3$ was shown (Figure 10f vs Figure 11f), indicating that the adsorption of EPCG toward Cu(II) was also an ion-exchange process. For the regenerated EPCG, the peaks of the binding energies from the XPS analysis were very similar to those of the original EPCG samples (Figure 10 vs Figure 12); especially the peak of the Cu $2p^3$ binding energy that was almost absent (Figure 10f vs Figure 12f). Furthermore, most of the adsorbed Cu(II) had been desorbed from the EPCG skeletons to realize the good regeneration of EPCG for recycling reuse.

3. CONCLUSIONS

When carrying out a cross-linking copolymerization of one strongly polar CMDA cross-linker and another common monomer of acrylic acid (AA) and then a simple neutralization treatment, it was surprisingly discovered that a new highly expanded polycarboxylate gel (EPCG) had been formed in the copolymerization system. When the EPCG was immersed in water, it could be quickly expanded 29.44 times to have a high permeability inside and realize the efficient adsorption toward Cu(II) in water.

The study was the first to use the highly expanded polycarboxylate gel (EPCG) as a new type of adsorbent for

https://dx.doi.org/10.1021/acsomega.0c05431
ACS Omega 2021, 6, 5318−5334

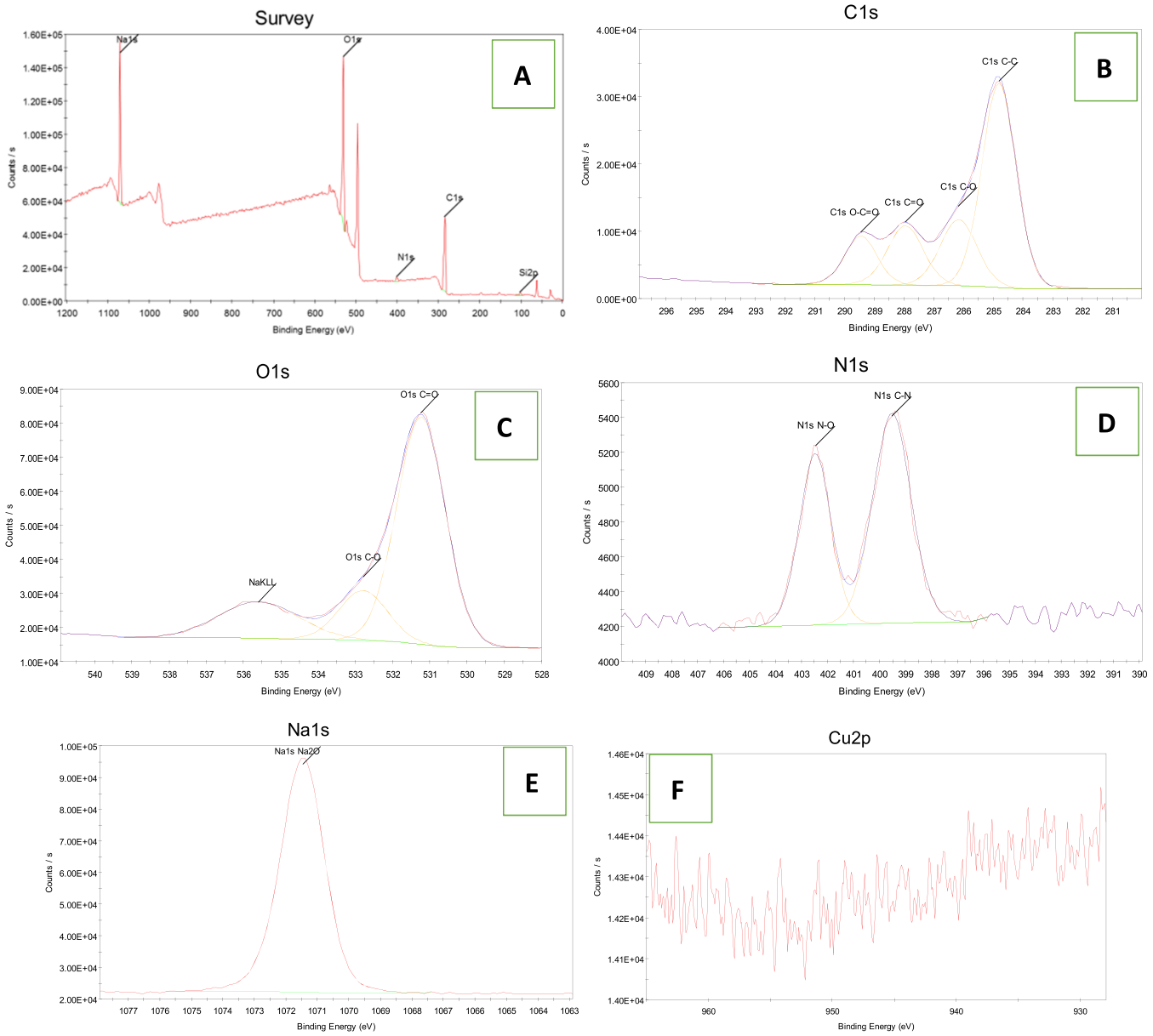

Figure 10. XPS analysis of the original EPCG samples. (A) Survey scanning of XPS analysis of the original EPCG samples. (b) Scanning the C 1s binding energies of the original EPCG samples. (c) Scanning the O 1s binding energies of the original EPCG samples. (D) Scanning the N 1s binding energies of the original EPCG samples. (E) Scanning the Na 1s binding energies of the original EPCG samples. (F) Scanning the Cu 2p binding energies of the original EPCG samples.

purifying Cu(II)-containing wastewater. The results showed that the adsorption capacity of EPCG toward Cu(II) was 261.70 mg/g, which was higher than that of all the selected existing adsorbents reported in recent years. The adsorption rate of expanded EPCG was 3.61 times higher than that of the previous polyantionic gel (PAG). An enlarged application of EPCG adsorption toward 4.0 L of a Cu(II)-containing solution had been successfully realized, confirming the good potentiality for this new EPCG adsorbent to be further applied in real engineering for purifying Cu(II)-containing wastewater.

Similarly, due to the high expansion and high permeability of EPCG, when the EPCG adsorbent was mixed with an alkaline NaOH solution, a novel NaOH-coated EPCG material was obtained, and its adsorption capacity toward Cu(II) had been further improved to 333.21 mg/g, which was higher than that of the pure EPCG adsorbent.

Moreover, in the acid conditions, the EPCG samples with saturated adsorption of Cu(II) could be fully desorbed to be regenerated for reuse. The Cu(II) desorption percentage (DR %) was 99.39%, i.e., 99.39% of the adsorbed Cu(II) could be desorbed from EPCG wastes to be recovered. The adsorption capacity of regenerated EPCG reused for adsorbing Cu(II) was 259.05 mg/g, which was very near that of the original EPCG, indicating that the EPCG adsorbent could be efficiently recycled for reuse in the purification of Cu(II)-containing wastewater.

In addition, a series of simulation experiments and instrumental analysis (i.e., FT-IR, XRD, SEM, and XPS) were adopted to confirm the new environmental response effects during the adsorption of EPCG toward Cu(II), including "expansion-shrink" response, "alkali-coating" response, and "acid-desorption" response. The new environ-

https://dx.doi.org/10.1021/acsomega.0c05431
ACS Omega 2021, 6, 5318−5334

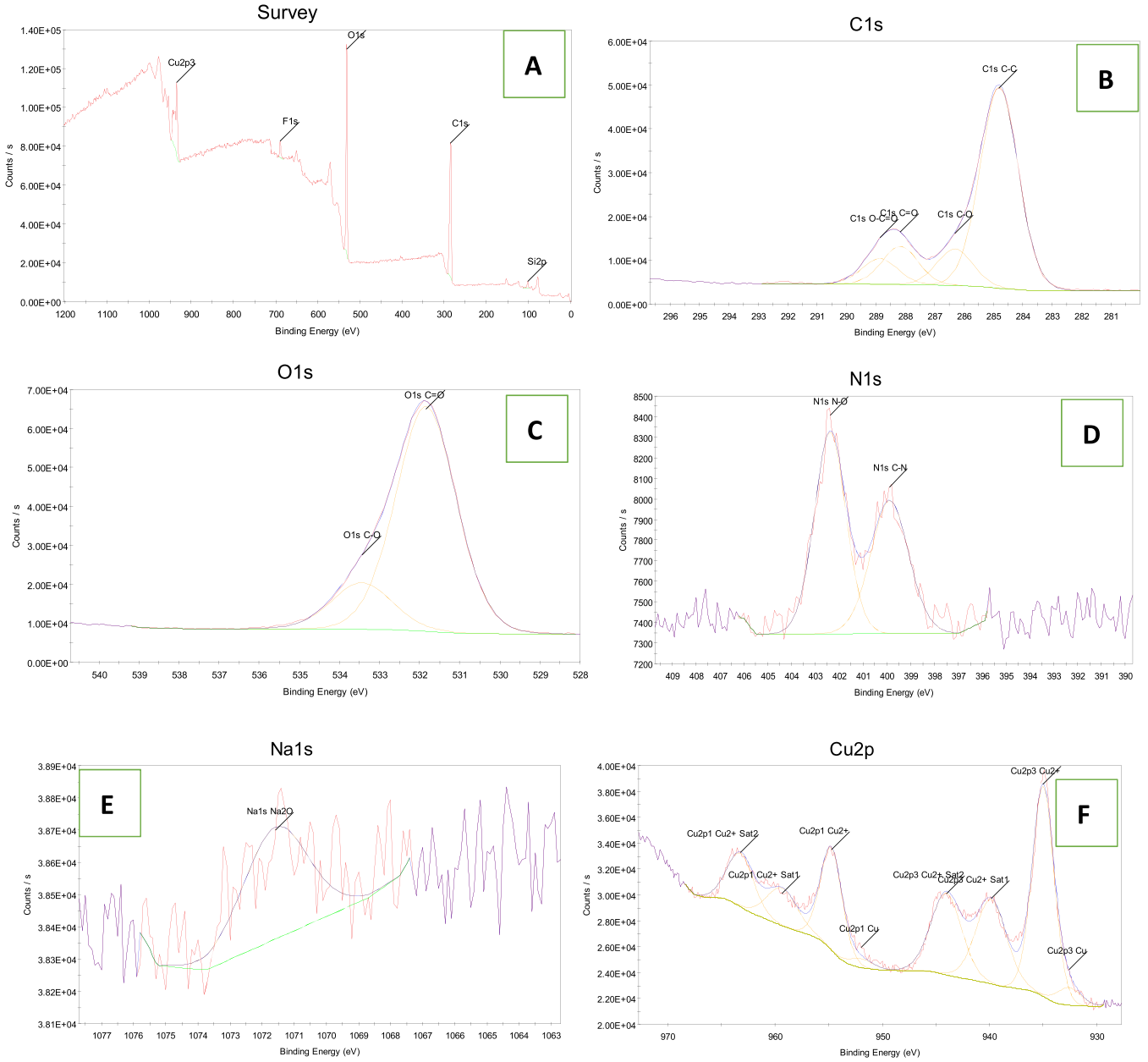

Figure 11. XPS analysis of the EPCG samples after adsorbing Cu(II). (A) Survey scanning of XPS analysis of the EPCG samples after adsorbing Cu(II). (b) Scanning the C 1s binding energies of the EPCG samples after adsorbing Cu(II). (c) Scanning the O 1s binding energies of the EPCG samples after adsorbing Cu(II). (d) Scanning the N 1s binding energies of the EPCG samples after adsorbing Cu(II). (e) Scanning the Na 1s binding energies of the EPCG samples after adsorbing Cu(II). (f) Scanning the Cu 2p binding energies of the EPCG samples after adsorbing Cu(II).

mental response effects were the key factors for the EPCG adsorbent to realize a more satisfactory adsorption toward Cu(II) than we could do before.

4. EXPERIMENTAL

4.1. Materials. 3-Chloro-2-hydroxypropylmethyldiallylammonium chloride (CMDA) was self-prepared by a quaternization condensation of methyldiallylamine and epichlorohydrin at 35 °C for 8 h based on our previously contributed synthesis process,[31] and the molecular structure of CMDA was confirmed by the FT-IR and ^{1}H NMR analysis technologies listed in the Supporting Information. Acrylic acid (AA) was of analytical purity (Shandong Qilu Chemical Co., Ltd., China). Ammonium persulfate (APS) (Yixing Tianpeng Fine Chemical Co., Ltd., China) and $CuSO_4$ (Zhejiang Jiaxing Qunfeng Chemical Co., Ltd., China) were the analytical reagents.

4.2. Synthesis of the EPCG Adsorbent. In a 100 mL round-bottomed flask, a reaction solution was formed by dissolving 14.2 g of AA, 2.1 g of DMAC, and 0.49 g of ammonium persulfate (APS, initiator) into 13.3 mL of deionized water. Subsequently, the reaction solution was warmed to 65 °C to run the cross-linking copolymerization for 0.5 h, and then the intermediate product was neutralized by 100 mL of 10% NaOH solution to obtain the optimal EPCG product with a molar ratio of DMAC and AA units of 5/95.

4.3. Adsorption Studies of EPCG Adsorbents. First, a series of isotherm adsorptions of 0.01−0.1 g of EPCG samples toward 50 mL of $CuSO_4$ solution with Cu(II) concentration of

https://dx.doi.org/10.1021/acsomega.0c05431
ACS Omega 2021, 6, 5318−5334

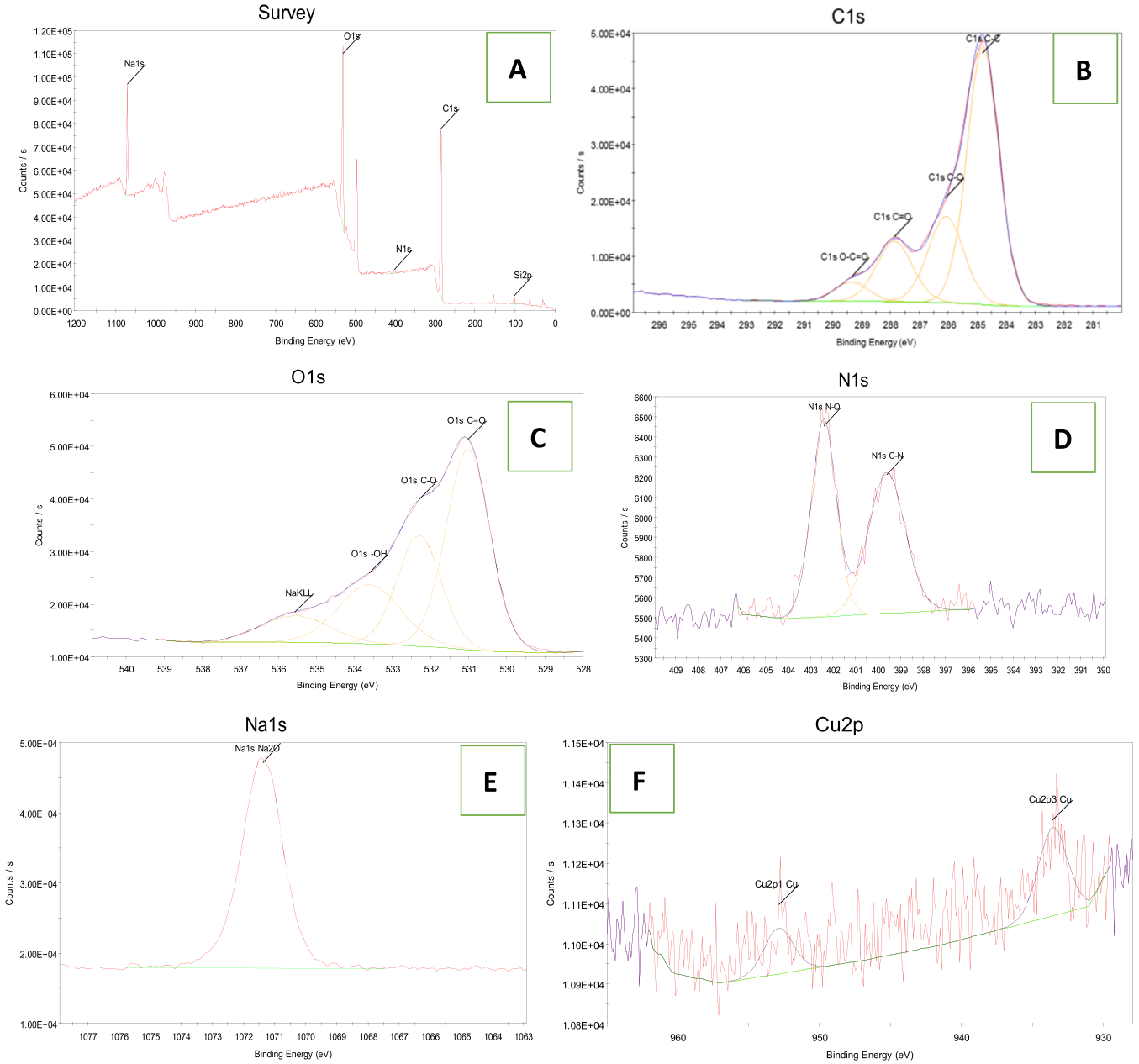

Figure 12. XPS analysis of the regenerated EPCG samples. (A) Survey scanning of XPS analysis of the regenerated EPCG samples. (b) Scanning the C 1s binding energies of the regenerated EPCG samples. (c) Scanning the O 1s binding energies of the regenerated EPCG samples. (d) Scanning the N 1s binding energies of the regenerated EPCG samples. (e) Scanning the Na 1s binding energies of the regenerated EPCG samples. (f) Scanning the Cu 2p binding energies of the regenerated EPCG samples.

10−2000 mg/L were carried out at 30−50 °C for 100 h. The residual Cu(II) concentrations in the supernatants after isotherm adsorptions were measured using a plasma optical emission spectrometer. The Cu(II) removal percentage (R%) and the adsorption capacity were selected to evaluate the adsorption results of EPCG. The Cu(II) removal percentage (R%) could be calculated using the following equation:

$$R\% = \frac{C_0 \bullet V_0 - C_1 \bullet V_1}{C_0 \bullet V_0} \times 100\% \quad (8)$$

where C_0 is the original Cu(II) concentration in the solution, V_0 is the volume of the original Cu(II)-containing solution. C_1 is the Cu(II) concentration in the solution after EPCG adsorption to reach the adsorption equilibrium, and $V_1$is the volume of the treated Cu(II)-containing solution.

The equilibrium adsorption capacities (q_e) could be calculated according to the following equation:

$$q_e = \frac{(C_0 - C_t) \times V}{m} \quad (9)$$

where V is the volume of the selected Cu(II)-containing solution and m is the mass of the used EPCG adsorbent.

In addition, a series of adsorption kinetics experiment of 0.3 g of EPCG samples toward 50 mL of $CuSO_4$ solution with Cu(II) concentrations of 10−2000 mg/L were conducted at 30 °C for 1−11 min with continuous stirring. The residual Cu(II) concentrations (C_t) at each time interval (t) were

https://dx.doi.org/10.1021/acsomega.0c05431
ACS Omega 2021, 6, 5318−5334

detected by a plasma optical emission spectrometer. The adsorption capacity (q_t) at time t could be calculated according to the following equation:

$$q_t = \frac{(C_0 - C_t) \times V}{m} \quad (10)$$

The related adsorption data (q_e, q_t) at different adsorption times (t) were substituted into the serial adsorption kinetics equations, e.g., the pseudo-first kinetics, pseudo-second kinetics, intraparticle diffusion, and particle diffusion equations, to evaluate the adsorption kinetics behaviors of EPCG.

4.4. Construction of the NaOH-coated EPCG System. Dry EPCG samples (0.3 g) were immersed into 100 mL of 2% (w/w) NaOH solution with continuous stirring at 90 °C for 30 min so that the NaOH regents could be permeated inside the expanded EPCG to be coated by EPCG skeletons, forming a novel NaOH-coated EPCG product. The NaOH-coated EPCG product was directly dried (without any washing) again at 80 °C for 8.0 h to be reserved for the purification of Cu(II)-containing wastewater.

4.5. Desorption of EPCG Samples after the Saturated Adsorption of Cu(II). At room temperature, 2.0 g of EPCG samples with the saturated adsorption of Cu(II) was stirred with a 50 mL of 1/1 (v/v) HCl solution for 100 h so that the adsorbed Cu(II) could be efficiently desorbed from the EPCG skeletons to be soluble in the HCl solution. The desorbed Cu(II) concentration in the HCl solution (C_d) was measured by a plasma optical emission spectrometer, and the Cu(II) desorption percentage (DR%) was calculated to evaluate the desorption results.

The EPCG samples after desorption were reneutralized with a 100 mL 10% NaOH solution to regenerate the EPCG adsorbents for reuse to adsorb the Cu(II)-containing solution and systemically evaluate the recyclability of EPCG.

■ ASSOCIATED CONTENT

Supporting Information

The Supporting Information is available free of charge at https://pubs.acs.org/doi/10.1021/acsomega.0c05431.

The FT-IR and ^{1}H NMR analysis results of 3-chloro-2-hydroxypropylmethyldiallylammonium chloride (CMDA) (Figures S1 and S2) (PDF)

■ AUTHOR INFORMATION

Corresponding Author

Yikai Yu − *College of Chemistry and Chemical Engineering, Jiangxi Normal University, Nanchang 330022, China; Key Laboratory of Chemical Biology of Jiangxi Province, Nanchang 330022, China;* orcid.org/0000-0003-0914-4070; Email: yuyikai1980@163.com

Authors

Hongyan Li − *College of Chemistry and Chemical Engineering, Jiangxi Normal University, Nanchang 330022, China*

Yu Bai − *College of Chemistry and Chemical Engineering, Jiangxi Normal University, Nanchang 330022, China*

Qiwen Yang − *College of Chemistry and Chemical Engineering, Jiangxi Normal University, Nanchang 330022, China*

Complete contact information is available at: https://pubs.acs.org/10.1021/acsomega.0c05431

Author Contributions

#H.L. and Y.B. contributed equally.

Notes

The authors declare no competing financial interest.

■ ACKNOWLEDGMENTS

This work was financially supported by the National Nature Science Foundation of China (Project No. 21866016).

■ REFERENCES

(1) Cao, D.; Cao, Z.; Wang, G.; Dong, X.; Dong, Y.; Ye, Y.; Hu, S. Plasma induced graft co-polymerized electrospun polyethylene terephalate membranes for removal of Cu^{2+} from aqueous solution. *Chem. Phys.* **2020**, *536*, 110832.

(2) Mokadem, Z.; Saidi-Besbes, S.; Lebaz, N.; Elaissari, A. Magnetic monolithic polymers prepared from high internal phase emulsions and Fe_3O_4 triazole-functionalized nanoparticles for Pb^{2+}, Cu^{2+} and Zn^{2+} removal. *React. Funct. Polym.* **2020**, *155*, 104693.

(3) Wang, L.; Li, J.; Wang, J.; Guo, X.; Wang, X.; Choo, J.; Chen, L. Green multi-functional monomer based ion imprinted polymers for selective removal of copper ions from aqueous solution. *J. Colloid Interface Sci.* **2019**, *541*, 376−386.

(4) Liu, J.; Hu, C.; Huang, Q. Adsorption of Cu^{2+}, Pb^{2+}, and Cd^{2+} onto oiltea shell from water. *Bioresour. Technol.* **2019**, *271*, 487−491.

(5) Mahmoud, M.; Khalifa, M.; Al-sherady, M.; Mohamed, A.; El-Demerdash, F. A novel multifunctional sandwiched activated carbon between manganese and tin oxides nanoparticles for removal of divalent metal ions. *Powder Technol.* **2019**, *351*, 169−177.

(6) Liu, Y.; Wang, R.; Bai, J.; Jiao, T.; Bai, Z.; Zhang, L.; Zhang, Q.; Zhou, J.; Peng, Q. Non-covalent self-assembly of multi-target polystyrene composite adsorbent with highly efficient Cu(II) ion removal capability. *Colloids Surf., A* **2019**, *577*, 674−682.

(7) Awual, M. R. Novel nanocomposite materials for efficient and selective mercury ions capturing from wastewater. *Chem. Eng. J.* **2017**, *307*, 456−465.

(8) Li, H.; Wang, Z.; Liu, X.; Cui, F.; Chen, C.; Zhang, Z.; Li, J.; Song, L.; Bai, R. Functionalised poplar catkins aerogels: Synthesis, characterisation and application to adsorb Cu(II) and Pb(II) from wastewater. *Chem. Phys. Lett.* **2020**, *755*, 137805.

(9) Liu, F.; Li, S.; Yu, D.; Su, Y.; Shao, N.; Zhang, Z. Template-Free Synthesis of Oxygen-Doped Bundlelike Porous Boron Nitride for Highly Efficient Removal of Heavy Metals from Wastewater. *ACS Sustainable Chem. Eng.* **2018**, *6*, 16011−16020.

(10) Maity, J.; Ray, S. K. Competitive Removal of Cu(II) and Cd(II) from Water Using a Biocomposite Hydrogel. *Phys. Chem. B* **2017**, *121*, 10988−11001.

(11) Wang, Y.; Wang, B.; Wang, Q.; Di, J.; Miao, S.; Yu, J. Amino-Functionalized Porous Nanofibrous Membranes for Simultaneous Removal of Oil and Heavy-Metal Ions from Wastewater. *ACS Appl. Mater. Interfaces* **2019**, *11*, 1672−1679.

(12) Thirumavalavan, M.; Lai, Y.-L.; Lin, L.-C.; Lee, J.-F. Cellulose-Based Native and Surface Modified Fruit Peels for the Adsorption of Heavy Metal Ions from Aqueous Solution: Langmuir Adsorption Isotherms. *Chem. Eng. Data* **2010**, *55*, 1186−1192.

(13) Maleki, A.; Hajizadeh, Z.; Sharifi, V.; Emdadi, Z. A green, porous and eco-friendly magnetic geopolymer adsorbent for heavy metals removal from aqueous solutions. *J. Cleaner Prod.* **2019**, *215*, 1233−1245.

(14) Wang, W.; Shu, G.; Tian, H.; Zhu, X. Removals of Cu(II), Ni(II), Co(II) and Ag(I) from wastewater and electricity generation by bimetallic thermally regenerative electro-deposition batteries. *Sep. Purif. Technol.* **2020**, *235*, 116230.

(15) Zhao, D.; Wang, Z.; Lu, S.; Shi, X. An amidoxime-functionalized polypropylene fiber: Competitive removal of Cu(II), Pb(II) and Zn(II) from wastewater and subsequent sequestration in cement mortar. *J. Cleaner Prod.* **2020**, *274*, 123049.

(16) Li, B.; Zheng, J. Q.; Guo, J. Z.; Dai, C. Q. A novel route to synthesize MOFs-derived mesoporous dawsonite and application in

elimination of Cu(II) from wastewater. *Chem. Eng. J.* **2020**, *383*, 123174.
(17) Su, Q.; Ye, Q.; Deng, L.; He, Y.; Cui, X. Prepared self-growth supported copper catalyst by recovering Cu (II) from wastewater using geopolymer microspheres. *J. Cleaner Prod.* **2020**, *272*, 122571.
(18) Jiang, Q.; Song, X.; Liu, J.; Shao, Y.; Feng, Y. In-situ Cu(II) enrichment and recovery from low-strength copper-laden wastewater using a novel electrically enhanced microbial copper recovery cell (MCRC). *Chem. Eng. J.* **2020**, *382*, 122788.
(19) Zhang, L.; Wu, B.; Gan, Y.; Chen, Z.; Zhang, S. Sludge reduction and cost saving in removal of Cu(II)-EDTA from electroplating wastewater by introducing a low dose of acetylacetone into the Fe(III)/UV/NaOH process. *J. Hazard. Mater.* **2020**, *382*, 121107.
(20) Ahmad, M.; Wang, J.; Xu, J.; Zhang, Q.; Zhang, B. Magnetic tubular carbon nanofibers as efficient Cu(II) ion adsorbent from wastewater. *J. Cleaner Prod.* **2020**, *252*, 119825.
(21) Shao, N.; Tang, S.; Liu, Z.; Li, L.; Yan, F.; Liu, F.; Li, S.; Zhang, Z. Hierarchically Structured Calcium Silicate Hydrate-Based Nanocomposites Derived from Steel Slag for Highly Efficient Heavy Metal Removal from Wastewater. *ACS Sustainable Chem. Eng.* **2018**, *6*, 14926−14935.
(22) Wang, H.; Wang, C.; Tao, S.; Qiu, J.; Yu, Y.; Gu, M. Biomimetic Preparation of Hybrid Porous Adsorbents for Efficiently Purifying Complex Wastewater. *ACS Sustainable Chem. Eng.* **2016**, *4*, 992−998.
(23) Ma, J.; Zhou, G.; Chu, L.; Liu, Y.; Liu, C.; Luo, S.; Wei, Y. Efficient Removal of Heavy Metal Ions with An EDTA Functionalized Chitosan/Polyacrylamide Double Network Hydrogel. *ACS Sustainable Chem. Eng.* **2017**, *5*, 843−851.
(24) Ge, Y.; Li, Z. Application of Lignin and Its Derivatives in Adsorption of Heavy Metal Ions in Water: A Review. *ACS Sustainable Chem. Eng.* **2018**, *6*, 7181−7192.
(25) Sharma, P. R.; Chattopadhyay, A.; Sharma, S. K.; Geng, L.; Amiralian, N.; Martin, D.; Hsiao, B. S. Nanocellulose from Spinifex as an Effective Adsorbent to Remove Cadmium(II) from Water. *ACS Sustainable Chem. Eng.* **2018**, *6*, 3279−3290.
(26) Cao, J.-S.; Wang, C.; Fang, F.; Lin, J.-X. Removal of heavy metal Cu(II) in simulated aquaculture wastewater by modified palygorskite. *Environ. Pollut.* **2016**, *219*, 924−931.
(27) Li, G.-P.; Zhang, K.; Zhang, P. F.; Liu, W.-N.; Tong, W.-Q.; Hou, L.; Wang, Y.-Y. Thiol-Functionalized Pores via Post-Synthesis Modification in a Metal−Organic Framework with Selective Removal of Hg(II) in Water. *Inorg. Chem.* **2019**, *58*, 3409−3415.
(28) Zhang, P.; Hou, D.; O'Connor, D.; Li, X.; Pehkonen, S.; Varma, R. S.; Wang, X. Green and Size-Specific Synthesis of Stable Fe−Cu Oxides as Earth-Abundant Adsorbents for Malachite Green Removal. *ACS Sustainable Chem. Eng.* **2018**, *6*, 9229−9236.
(29) Lv, D.; Liu, Y.; Zhou, J.; Yang, K.; Lou, Z.; Baig, A.; Xu, X. Application of EDTA-functionalized bamboo activated carbon (BAC) for Pb(II) and Cu(II) removal from aqueous solutions. *Appl. Surf. Sci.* **2018**, *428*, 648−658.
(30) Song, C.; Li, H.; Yu, Y. Homologous-heterogeneous Structure Control and Intelligent Adsorption Effect of A Polycationic Gel for Super-efficient Purification of Dyeing Wastewater. *RSC Adv.* **2019**, *9*, 9421−9434.
(31) Jia, Q.; Song, C.; Li, H.; Huang, Y.; Liu, L.; Yu, Y. Construction of polycationic film coated cotton and new inductive effect to remove water-soluble dyes in water. *Mater. Des.* **2017**, *124*, 1−15.
(32) Song, C.; Zhao, J.; Li, H.; Liu, L.; Li, X.; Huang, X.; Liu, H.; Yu, Y. One-Pot Synthesis and Combined Use of Modified Cotton Adsorbent and Flocculant for Purifying Dyeing Wastewater. *ACS Sustainable Chem. Eng.* **2018**, *65*, 6876−6888.
(33) Song, C.; Yu, Y.; Sang, X. Synthesis and Surface Gel-adsorption Effect of Multidimensional Cross-linking Cationic Cotton for Enhancing Purification of Dyeing Waste-water. *J. Chem. Technol. Biotechnol.* **2019**, *94*, 120−127.
(34) Song, C.; Li, H.; Yu, Y. Synthesis, microstructure transformations, and long-distance inductive effectof poly-(acrylethyltrimethylammonium chloride) cotton with super-high adsorption ability for purifying dyeing wastewater. *Cellulose* **2019**, *26*, 3987−4004.
(35) Li, H.; Zhao, J.; Bai, Y.; Song, C.; Yu, Y. Switch effect, water-like state, and new interaction mechanism of an H-bonded polycation-polyacrylamide system to realize instant decolorization of dyeing wastewater. *Adv. Sustain. Syst.* **2019**, *3*, 1900029.
(36) Li, H.; Song, C.; Bai, Y.; Yu, Y. A facilely synthesized polyanionic gel adsorbent with high adaptability and new adsorption effects for purification of Cu(II)-containing wastewater. *J. Chem. Technol. Biotechnol.* **2019**, *94*, 3661−3675.
(37) Bai, Y.; Song, C.; Li, H.; Yang, Q.; Yu, Y. A facilely-synthesized, highly-permeable, and efficiently-recyclable polycationic gel with cohesive state transformations for purifying dyeing wastewater. *ACS Omega* **2020**, *5*, 8046−8055.
(38) Cheng, H.; Li, Y.; Wang, B.; Mao, Z.; Xu, H.; Zhang, L.; Zhong, Y.; Sui, X. Chemical crosslinking reinforced flexible cellulose nanofiber-supported cryogel. *Cellulose* **2018**, *25*, 573−582.
(39) Wang, X.; Lou, Y.; Ye, X.; Chen, X.; Fang, L.; Zhai, Y.; Zheng, Y.; Xiong, C. Green chemical method for the synthesis of chromogenic fifiber and its application for the detection and extraction of Hg^{2+} and Cu^{2+} in environmental medium. *J. Hazard. Mater.* **2019**, *364*, 339−348.
(40) Haan, T. Y.; Ming, K. L.; Mohammad, A. W. Synthesis of Cellulose Hydrogel for Copper (II) Ions Adsorption. *J. Environ. Chem. Eng.* **2018**, *6*, 4588−4597.
(41) Hoang, A. T.; Bui, X. L.; Pham, X. D. A novel investigation of oil and heavy metal adsorption capacity from as-fabricated adsorbent based on agricultural by-product and porous polymer. *Energy Source Part, A* **2018**, *40*, 929−939.
(42) Sudha, R.; Srinivasb, B.; Gouru, N. K.; Ramesha, K. Removal of copper by adsorption on treated laterite. *Mater. Today:Proc.* **2018**, *5*, 463−469.
(43) Surgutskaia, N.; Di, M. A.; Zednik, J.; Ozaltin, K.; Lovecka, L.; Bergerova, E.; Kimmer, D.; Svoboda, J.; Sedlarik, V. Efficient Cu^{2+}, Pb^{2+} and Ni^{2+} ion removal from wastewater using electrospun DTPA-modified chitosan/polyethylene oxide nanofibers. *Sep. Purif. Technol.* **2020**, *247*, 116914.
(44) Awual, M. R.; Hasan, M. M.; Rahman, M. M.; Asiri, A. M. Novel composite material for selective copper(II) detection and removal from aqueous media. *J. Mol. Liq.* **2019**, *283*, 772−780.
(45) Elshaarawy, R. F. M.; el-Abd, H. A.; Hegazy, W.; Mustafa, F.; Talkhan, T. Poly(ammonium/pyridinium)-chitosan Schiff base as a smart biosorbent for scavenging of Cu2+ ions from aqueous effluents. *Polym. Test.* **2020**, *83*, 106244.
(46) Ali, M. B.; Wang, F.; Boukherroub, R.; Xia, M. High performance of phytic acid-functionalized spherical poly-phenylglycine particles for removal of heavy metal ions. *Appl. Surf. Sci.* **2020**, *518*, 146206.
(47) Awuala, M. R. Novel ligand functionalized composite material for efficient copper(II) capturing from wastewater sample. *Compos. Part B-Eng.* **2019**, *172*, 387−396.
(48) Qi, X.; Liu, R.; Chen, M.; Li, Z.; Qin, T.; Qian, Y.; Zhao, S.; Liu, M.; Zeng, Q.; Shen, J. Removal of copper ions from water using polysaccharide-constructed hydrogels. *Carbohydr. Polym.* **2019**, *209*, 101−110.
(49) Xie, Y.; Yuan, X.; Wu, Z.; Zeng, G.; Jiang, L.; Peng, X.; Li, H. Adsorption behavior and mechanism of Mg/Fe layered double hydroxide with Fe_3O_4-carbon spheres on the removal of Pb(II) and Cu(II). *J. Colloid Interface Sci.* **2019**, *536*, 440−455.
(50) Zhang, D.; Li, H.; Li, J.; Xu, Z.; Liu, H.; Zhao, Y.; Feng, X.; Chen, L. Hydrophilic P(Am-CD-AMPS) microgel for visual detection and removal metal ions in aqueous solution. *Appl. Surf. Sci.* **2020**, *512*, 145668.
(51) Chen, C.; Li, F.; Guo, Z.; Qu, X.; Wang, J.; Zhang, J. Preparation and performance of aminated polyacrylonitrile nanofibers for highly efficient copper ion removal. *Colloids Surf., A* **2019**, *568*, 334−344.

https://dx.doi.org/10.1021/acsomega.0c05431
ACS Omega 2021, 6, 5318−5334

(52) Awuala, M. R. New type mesoporous conjugate material for selective optical copper(II) ions monitoring & removal from polluted waters. *Chem. Eng. J.* **2017**, *307*, 85−94.
(53) Qiu, X.; Hu, H.; Yang, J.; Wang, C.; Cheng, Z. Removal of trace copper from simulated nickel electrolytes using a new chelating resin. *Hydrometallurgy* **2018**, *180*, 121−131.
(54) Hoslett, J.; Ghazal, H.; Ahmad, D.; Jouhara, H. Removal of copper ions from aqueous solution using low temperature biochar derived from the pyrolysis of municipal solid waste. *Sci. Total Environ.* **2019**, *673*, 777−789.
(55) Cao, M.-l.; Lia, Y.; Yin, H.; Shen, S. Functionalized graphene nanosheets as absorbent for copper (II) removal from water. *Ecotoxicol. Environ. Safety* **2019**, *173*, 28−36.
(56) Li, X.; Deng, G.; Zhang, Y.; Wang, J. Rapid removal of copper ions from aqueous media by hollow polymer nanoparticles. *Colloids Surf., A* **2019**, *568*, 345−355.
(57) Zhou, L.; Li, N.; Owens, G.; Chen, Z. Simultaneous removal of mixed contaminants, copper and norfloxacin, from aqueous solution by ZIF-8. *Chem. Eng. J.* **2019**, *362*, 628−637.
(58) Jung, K. W.; Lee, S. Y.; Choi, J. W.; Lee, Y. J. A facile one-pot hydrothermal synthesis of hydroxyapatite/biochar nanocomposites: Adsorption behavior and mechanisms for the removal of copper(II) from aqueous media. *Chem. Eng. J.* **2019**, *369*, 529−541.
(59) da Silva, A. J. F.; Moura, M. C. P. A.; Santos, E. S.; Pereira, J. E. S.; de Barros Neto, E. L. Copper removal using carnauba straw powder: Equilibrium, kinetics, and thermodynamic studies. *J. Environ. Chem. Eng.* **2018**, *6*, 6828−6835.
(60) Milagres, J. L.; Bellato, C. R.; Vieira, R. S.; Ferreir, S. O.; Reis, C. Preparation and evaluation of the Ca-Al layered double hydroxide for removal of copper(II), nickel(II), zinc(II), chromium(VI) and phosphate from aqueous solutions. *J. Environ. Chem. Eng.* **2017**, *5*, 5469−5480.

https://dx.doi.org/10.1021/acsomega.0c05431
ACS Omega 2021, 6, 5318−5334